Article

Potential Sustainable Edible Packaging from Chickpea Starch–Alginate Bioplastic

Md Abdur Rahim Badsha [1], Brooklyn Weiers [1], Lexi Hoeft [1], Michael Kjelland [1], Israt Zaman [2], Khwaja Hossain [1,*]

[1] Division of Science and Mathematics, Mayville State University, Mayville, ND 58257, USA; mdabdurrahim.badsha@mayvillestate.edu (MARB); brooklyn.weiers@mayvillestate.edu (BW); lexi.hoeft@mayvillestate.edu (LH); michael.kjelland@mayvillestate.edu (MK)

[2] Department of Plant Pathology, Microbiology, and Biotechnology, North Dakota State University, Fargo, ND 58102, USA; israt.zaman@ndus.edu (IZ)

* Correspondence: Khwaja Hossain, Email: k.hossain@mayvillestate.edu; Tel.: +1-70-179-979-92.

ABSTRACT

Edible and biodegradable polymer films have emerged as promising alternatives to petroleum-based plastics because of their renewability, sustainability, and reduced environmental impact. In this study, potential edible bio-based films were developed from chickpea starch (CPS), sodium alginate (SA), and glycerol through gelatinization followed by solution casting. A CPS:SA: glycerol formulation of 1:1:3, containing 5 wt% calcium chloride ($CaCl_2$) relative to CPS, was prepared to improve film performance through ionic crosslinking. We hypothesized that calcium chloride crosslinking would enhance film cohesion, mechanical performance, thermal stability, and moisture barrier properties while maintaining potential edibility. The films' physicochemical, mechanical, thermal, and barrier properties were characterized using Fourier-transform infrared spectroscopy (FTIR), scanning electron microscopy (SEM), thermogravimetric analysis (TGA), tensile testing, transparency analysis, water vapor permeability (WVP), and film density measurements. FTIR analysis confirmed intermolecular interactions among chickpea starch, sodium alginate, and calcium ions, while SEM revealed a relatively homogeneous and compact film morphology. TGA (degradation starts at 270 °C) demonstrated enhanced thermal stability of the film. The optimized formulation exhibited a tensile strength of 13 MPa, elongation at break of 300%, Young's modulus of 10 MPa, transparency of 2.3%, and water vapor permeability of 8.66×10^{-14} g·day^{-1}·m^{-1}·Pa^{-1}. These results demonstrate that $CaCl_2$-crosslinked chickpea starch–alginate films possess a favorable balance of flexibility, structural integrity, thermal stability, and barrier performance. Although the edibility and safety of the developed films were not experimentally evaluated, the constituent materials used in this study are edible and generally recognized as safe. Therefore, these bio-based films have the potential to serve as promising

Open Access

Received: 24 Aug 2026
Accepted: 16 Nov 2026
Published: 27 Nov 2026

Copyright © 2026 by the author. Licensee Hapres, London, United Kingdom. This is an open access article distributed under the terms and conditions of Creative Commons Attribution 4.0 International License.

alternatives to conventional petroleum-based plastics for sustainable edible packaging and related applications.

KEYWORDS: chickpea starch; potential edible bioplastics; sustainable packaging; biodegradable polymers; green materials; film characterization

ABBREVIATIONS

CPS, Chickpea starch; EAB, Elongation break; FTIR, Fourier-transform infrared spectroscopy; SA, Sodium alginate; SEM, Scanning electron microscopy; TGA, Thermogravimetric analysis; TS, Tensile strength; WVP, Water vapor permeability; WCA, Water contact angle; YM, Young's modulus

INTRODUCTION

The widespread use of petroleum-based plastics has resulted in severe environmental challenges, including long-term persistence in ecosystems, accumulation of plastic waste in terrestrial and marine environments, and generation of microplastics that create risks to human health and biodiversity. As a result, there has been increasing demand for developing biodegradable and renewable alternatives to conventional plastics [1–5].

Among the emerging solutions, edible and biodegradable films have attracted significant attention as sustainable packaging materials. These films are designed to reduce plastic waste while maintaining essential functional properties such as moisture control, oxygen barrier performance, and mechanical protection of food products. In addition, edible films can be consumed directly or degrade naturally after disposal, making them environmentally friendly alternatives to synthetic packaging materials [6–8]. Widely used edible plastics are polysaccharide-based biopolymers because of their abundance, biodegradability, and film-forming ability [9].

Starch is one of the most extensively studied biopolymers for edible film fabrication due to its low cost, renewability, and biodegradability. Starch-based films have been widely investigated for packaging applications because of oxygen barrier properties and ease of processing [10,11]. However, native starch films suffer from several limitations, including poor mechanical strength, high brittleness, and strong hydrophilicity, which result in high water vapor permeability and reduced structural stability under humid conditions. Therefore, starch is often modified or blended with other biopolymers to improve its performance in practical applications.

One of the most commonly used raw materials in bioplastic production is corn starch due to its large-scale availability and established industrial processing. However, its use raises concerns regarding competition with food supply chains and sustainability. Moreover, corn starch-based films

often exhibit high water sensitivity and limited mechanical robustness [12]. Consequently, alternative starch sources from underutilized crops are receiving increasing attention for the development of sustainable and high-performance biodegradable materials.

Chickpea (*Cicer arietinum L.*) is the third most widely produced pulse crop globally and is an important source of carbohydrates, protein, and dietary fiber. Chickpea starch has been reported to contain a relatively higher amount of amylose among other cereals, which contributes to improved film-forming ability and stronger intermolecular interactions within polymer matrices [13,14]. In addition, the utilization of chickpea-based resources supports agricultural valorization and circular bioeconomy approaches by converting underutilized biomass into high-value functional materials [15].

To overcome the limitations of starch-based films, blending with complementary biopolymers is a widely used strategy. Sodium alginate, a naturally occurring anionic polysaccharide, has gained significant attention due to its biodegradability, non-toxicity, biocompatibility, and excellent gel-forming property [16,17]. Alginate-based films typically exhibit better transparency and oxygen barrier properties; however, they often show poor water resistance and moderate mechanical strength when used alone [17]. Therefore, blending starch with alginate offers a promising alternative for improving film performance by combining the advantages of both biopolymers.

The functional properties of alginate-based films can be significantly enhanced through ionic crosslinking with divalent cations such as calcium ions. A widely used food-grade crosslinking agent is Calcium chloride ($CaCl_2$) because Ca^{2+} ions interact with the guluronic acid blocks of alginate chains, forming a stable network [18–21]. This ionic crosslinking reduces polymer chain mobility, enhances intermolecular interactions, improves mechanical strength, and decreases solubility and permeability. Previous studies have demonstrated that Ca^{2+} crosslinking significantly influences the structural, thermal, and barrier properties of polysaccharide-based films [19,20].

Despite extensive research on starch-based and alginate-based edible films, limited studies focused on chickpea starch–sodium alginate composite films crosslinked with calcium chloride, particularly in terms of structure–property relationships. Most existing studies have examined either starch or alginate systems individually, while fewer have systematically investigated their synergistic interactions in the presence of ionic crosslinking. Furthermore, comprehensive evaluation of mechanical, thermal, morphological, and barrier properties in such systems remains inadequately explored [22].

This study developed potential bio-based films from chickpea starch and sodium alginate crosslinked with calcium chloride via solution casting. The films were comprehensively characterized using FTIR, SEM, TGA, tensile testing, transparency, water vapor permeability (WVP), and density

analyses. It was hypothesized that Ca^{2+}-induced ionic crosslinking would strengthen intermolecular interactions within the polymer matrix, thereby enhancing the films' mechanical, thermal, and barrier properties while preserving their potential biodegradability and edibility for sustainable food packaging applications [23].

MATERIALS AND METHODS

Materials and Experimental Procedures

Materials and Chemicals

Chickpeas were collected from the local market; sodium alginate (SA)and glycerol (plasticizer) were purchased from Thermo Scientific (Waltham, MA, USA). Potassium hydroxide (KOH) was obtained from Fisher Chemical (Gell, Belgium). Copper (II) sulfate pentahydrate ($CuSO_4 \cdot 5H_2O$; blue vitriol), was obtained from Fisher Scientific (Waltham, MA, USA). Anhydrous Calcium chloride ($CaCl_2$) was obtained from Sigma Aldrich (St. Louis, MO, USA). Cellulose nanocrystal (CNC) was purchased from Nanografi Advanced Materials (Ankara, Turkey). Commercially available polyethylene shopping bags and Ziploc sandwich bags obtained from Walmart were used as reference plastic materials.

Extraction of Starch from Chickpea

Chickpea starch was extracted following a wet-milling method based on our previously reported procedures and those of other researchers [24–26]. Dried chickpea seeds were purchased from a local market and sun-dried before processing. The dried seeds were milled into a fine powder using an electric grain mill grinder (2000 W high-speed grinder, Amazon, USA). The resulting chickpea flour was stored in an airtight container until further extraction.

For starch extraction, chickpea flour was dispersed in distilled water at a flour-to-water ratio of 1:10 (w/v) in a glass beaker. The suspension was continuously stirred at 300 rpm for 30 min at room temperature (27 °C) to facilitate hydration of the flour matrix and release of starch granules. The resulting slurry solution was kept at 4 °C overnight to allow starch granules to sediment by gravity.

After sedimentation, the upper aqueous phase containing soluble proteins, fibers, and other soluble components was carefully decanted. The remaining sediment was collected as crude starch. To improve starch recovery, the residual chickpea flour fraction was subjected to a second extraction cycle using the same water dispersion and sedimentation procedure.

From the starch suspension, starch was collected by centrifugation at 8885 g for 15 min. After centrifugation, the compact starch pellet was separated from the supernatant. The starch pellet was washed several times with distilled water until a clear supernatant was obtained to

remove residual impurities. The purified starch was then collected and dried in an oven at 35 °C until a constant weight was obtained.

The dried starch cake was gently ground into a fine powder with a mortar and pestle, then passed through a fine-mesh sieve. The extracted chickpea starch powder was stored in sealed polyethylene bags or airtight containers under dry conditions at room temperature for subsequent bio-based film preparation and characterization. The repeated extraction procedure resulted in an overall starch recovery of approximately 30 ± SD 2.15% (dry basis). The starch yield was calculated using the following formula.

$$\text{Starch Yield (\%)} = \frac{\text{Weight of dried starch}}{\text{Weight of dried chickpea}} \quad (1)$$

to ensure reproducibility, the extraction was performed independently ten times, and the starch yield was determined from the cumulative mass of chickpea powder processed and the corresponding total mass of dried starch recovered. A flow diagram of the starch extraction procedure is presented in Figure 1.

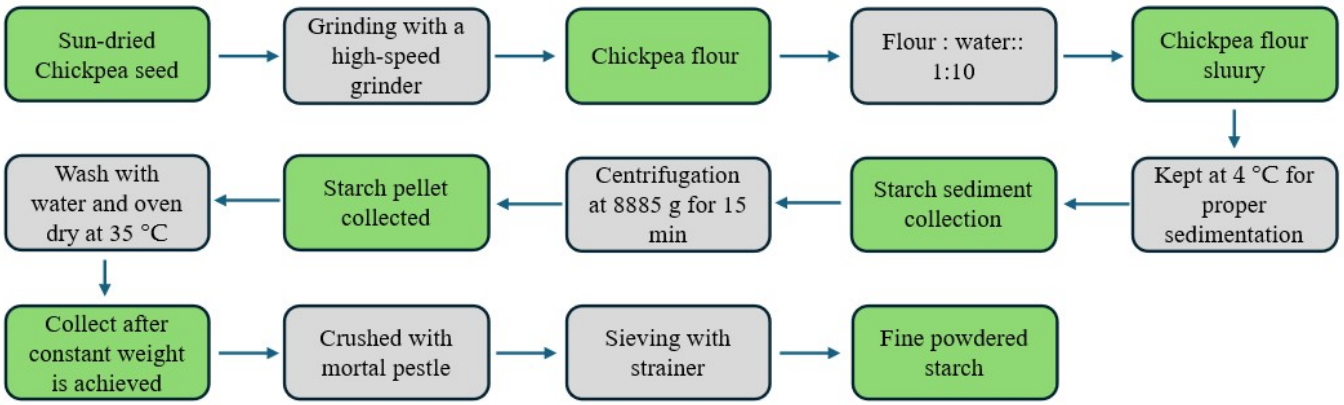


Figure 1. Schematic flow chart of starch extraction process.

Fabrication of Ion-Modified Starch/Sodium Alginate Biofilm

The bio-based films were prepared using a modified solution-casting method adapted from Mendes et al. (2023) [27]. Depending on the formulation, a suspension containing calcium chloride ($CaCl_2$) and cellulose nanocrystals (CNC) was first prepared in distilled water. The concentrations of both $CaCl_2$ and CNC were maintained at 5 wt% based on the dry weight of chickpea starch separately. Two hundred fifty milligrams of calcium chloride were taken in 100 mL distilled water. The suspension was magnetically stirred until a homogeneous mixture was obtained, after which the remaining film-forming components were added.

Five gm of extracted chickpea starch was gradually dispersed into the prepared suspension under continuous magnetic stirring (750 rpm), then heated to 80 °C for 20 min to promote complete starch gelatinization. Fifteen g of glycerol was subsequently incorporated as a plasticizer,

followed by the sequential addition of sodium alginate (SA) 5 g in total. The mixture was continuously stirred at 80 °C for 2 h to obtain a uniform, highly viscous polymeric slurry about 20 g. During this process, calcium ions interacted with the alginate chains through ionic crosslinking, while the CNCs were uniformly dispersed within the polymer matrix to reinforce the composite structure.

The resulting biopolymer slurry was poured into leveled glass Petri dishes (0.0038 m^2 of perimeter) and spread uniformly by gentle rotation. The films were dried in an oven at 60 °C overnight to ensure complete evaporation of the solvent and formation of uniform bio-based films. The dried films were carefully peeled from the casting plates and stored in airtight polyethylene bags in a dry environment until further analysis. The film obtained was 2 g. Film density of each formulation is shown in Table 1.

Table 1. Film density.

Sample title	Volume (cm^3)	Mass (g)	Density (g/cm^3)
CPSCa 1:1:3	0.877	1.117	1.274 ± 0.14
CPSCNC 1:1:3	0.856	1.041	1.217 ± 0.16
CPS 1:1:3	0.711	0.661	0.930 ± 0.12

A schematic illustration of the bio-based film preparation process is shown in Figure 2. The bio-based film formulations were prepared using different proportions of chickpea starch (CPS), sodium alginate (SA), and glycerol, with calcium chloride ($CaCl_2$) and cellulose nanocrystals (CNC) incorporated as additives. The composition of each formulation is summarized in Table 2.

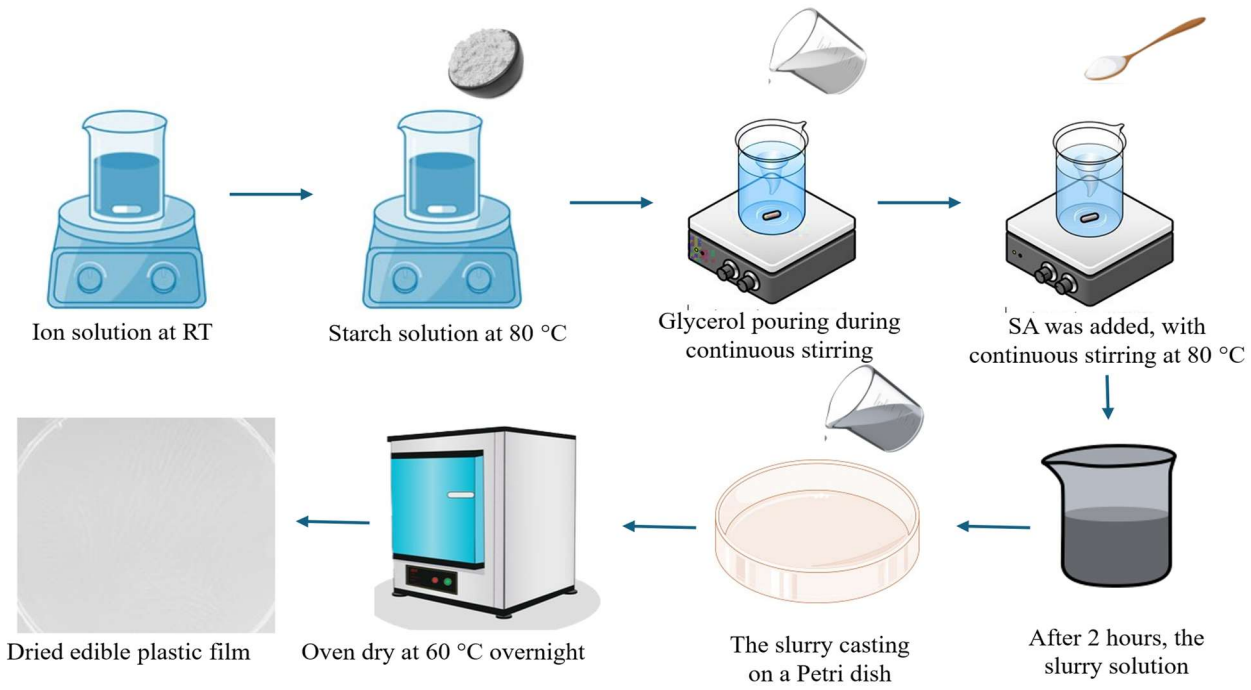


Figure 2. Schematic diagram of the film casting process.

Table 2. Formulation ratios of the chickpea starch-based bioplastic film.

Title	Chickpea extracted starch (CPS) (gm)	Sodium Alginate (SA) (gm)	Glycerol (gm)	Calcium chloride ($CaCl_2$) (gm)	Cellulose nanocrystals (CNC) (gm)	Proportion of the formulations (CPS:SA:Gly)
SA control	-	5	15	-	-	1:3
CPS 1:1:3	5	5	15	-	-	1:1:3
CPSCa 1:1:3	5	5	15	0.25 (5% to CPS)	-	1:1:3
CPSCNC 1:1:3	5	5	15	-	0.25 (5% to CPS)	1:3:3

Analytical Methods

FTIR Analysis

Fourier transform infrared (FTIR) spectroscopy was performed to investigate the chemical structure, functional groups, and intermolecular interactions of the extracted chickpea starch and all prepared bio-based film formulations. The spectra were recorded using an FTIR spectrometer (Nicolet iS5, Thermo Scientific, Waltham, MA, USA). Spectra were collected over the wavenumber range of 4000–650 cm^{-1}, with transmittance (%) plotted as a function of absorption frequency (cm^{-1}). The measurements were acquired using an incidence angle of 45°, a 2 mm sampling area, 16 background scans, an optical resolution of 0.8 cm^{-1}, and a data spacing of 0.06 cm^{-1} [27,28]. The resulting spectra were analyzed to identify the characteristic absorption bands of chickpea starch, sodium alginate, glycerol, calcium chloride, and cellulose nanocrystals, as well as to evaluate changes in peak position and intensity associated with hydrogen bonding, Ca^{2+}-mediated ionic crosslinking, and polymer–filler interactions within the composite bio-based films.

SEM Analysis

The surface morphology of the extracted chickpea starch and the prepared bio-based films formulations was examined using a JEOL JSM-6490LV scanning electron microscope. Before imaging, bio-based film specimens were cut to appropriate dimensions and mounted onto aluminum stubs with conductive silver paint. The mounted samples were sputter-coated with a thin gold layer using a Cressington 108Auto sputter coater to improve electrical conductivity and minimize charging during imaging. Scanning electron micrographs were acquired at accelerating voltages of 15 kV and varying magnifications to evaluate surface morphology, microstructural homogeneity, and the dispersion of the reinforcing components within the polymer matrix.

Mechanical Property Analysis

The mechanical properties of the prepared bio-based films were evaluated using a universal testing machine (Instron Model 5542, Instron Corporation, Norwood, MA, USA) in accordance with ASTM D412 [29]. Film specimens were cut into a rectangular-shaped geometry with an average gauge length of 4 cm. The specimens were mounted between the machine

grips and tested at a constant crosshead speed of 20 mm · min^{-1} until failure. Tensile strength (TS), elongation at break (EAB), and Young's modulus (YM) were determined from the resulting stress–strain curves. The EAB was calculated as the percentage increase in the gauge length at the point of fracture relative to the initial gauge length. For each formulation, three specimens were cut from a single film for analysis. These specimens were considered technical replicates and were not treated as independent film preparations.

Thermal Stability Analysis

The crystalline structure of the extracted chickpea starch and the prepared bio-based films was characterized using a TGA 550 Serial Number 0550-1291 thermogravimetric analyzer at North Dakota State University. The experiment was run under a nitrogen atmosphere at a heating rate of 10 °C/min to 600 °C for approximately 40 g of sample in a platinum HT pan.

Water Vapor Permeability Testing

The water vapor permeability (WVP) of the prepared bio-based films was evaluated using a modified gravimetric desiccant cup method ASTM E96 [30,31]. Briefly, 10 g of anhydrous calcium chloride ($CaCl_2$) as a desiccant was placed in a 50 mL glass beaker, which served as the desiccant chamber. The mouth of the 50 mL beaker was tightly sealed with the bio-based film specimen to prevent moisture leakage around the edges. The assembled unit was weighed to obtain its initial mass.

The sealed beaker was then placed inside a 1000 mL glass beaker containing 100 mL of distilled water at the bottom to create a humid environment. The large beaker was covered to maintain a constant humidity gradient and kept at room temperature (27 ± 2 °C) throughout the experiment. Under these conditions, water vapor diffused through the bio-based film and moisture was absorbed by the anhydrous $CaCl_2$, resulting in an increase in the mass of the sealed assembly. The assembly was removed at predetermined time intervals and weighed using an analytical balance. The cumulative mass gain was plotted as a function of time, and the water vapor transmission rate (WVTR) was determined from the slope of the linear region of the mass gain versus time curve by using the following formula,

$$\text{WVTR} = \frac{\Delta M}{\Delta t.A} = \frac{g}{day.\ m^2} \quad (2)$$

$$\text{Permeance} = \frac{\text{WVTR}}{\Delta P} = \frac{g}{s.\ m^2.Pa} \quad (3)$$

$$\text{WVP} = \text{permeance. Thickness} \quad (4)$$

$$\Delta M = M - M_0 \quad (5)$$

$$A = \pi r^2 \quad (6)$$

where M_0= initial mass (g), M= mass after moisture absorption (g), ΔM = weight gain (g), A = exposed film area (m^2), t = time (days), r = radius of the exposed bio-based films (m).

Water Contact Angle

The water contact angle (WCA) of the prepared bio-based films, followed by ASTM D7224-08, was measured to evaluate their surface wettability and hydrophobicity. Film specimens were cut into flat sections and placed on a clean glass slide at room temperature (25 ± 2 °C). A 5 µL droplet of distilled water was carefully deposited onto the film surface using a micropipette fitted with a 0.525 mm needle. Images of the water droplets were captured immediately after 5 s of deposition using a pluggable USB 2.0 digital microscope at 200× resolution (Model: USB2-MICRO-250X, Brand: Plugable, purchased from Amazon.com). The contact angle was determined using ImageJ software (version 1.54g) [32]. A total of 5 images were acquired at different places for each specimen to determine the average contact angle ± standard deviation, and the highest-quality image was selected for presentation [33–35]. For comparison, commercially available Ziploc sandwich bag and polyethylene bags purchased from a local Walmart store and they were analyzed under identical experimental conditions as reference materials.

Film Transparency

The optical transparency of the prepared bio-based films was evaluated using a modified spectrophotometric method based on previously reported procedures. Film specimens were cut into rectangular pieces (1 cm × 3 cm) to match the dimensions of a standard quartz cuvette. Each film sample was carefully attached to the inner wall of the cuvette to ensure a uniform optical path during measurement [36].

The percentage transmittance (%T) of the bio-based films was directly measured at 665 nm using a GENESYS™ 10S UV–VIS spectrophotometer (Thermo Scientific, USA). Measurements were performed under two different conditions: (i) an empty cuvette without abio-based film sample (reference baseline), (ii) an empty cuvette with the bio-based film attached to the cuvette wall. A polyethylene film and Ziploc sandwich bag sample were used as commercial plastic references for comparison. For each measurement, the cuvette was placed in the spectrophotometer, and the transmitted light intensity was recorded directly as percentage transmittance (%T). The transparency value of each film was calculated according to the following equation.

$$\text{Transparency} = \frac{log\ \%T}{b} \quad (7)$$

where T = transmittance at 665 nm, and b = thickness of the bio-based film in millimeters.

Statistical Analysis

Statistical analyses were performed using R. Linear regression models were used to evaluate differences among film formulations in tensile strength (TS), elongation at break (EAB), Young's modulus (YM), water contact angle (WCA), and water vapor permeability (WVP), with film formulation included as a categorical predictor and the control formulation as the reference group. Model significance was assessed using analysis of variance (ANOVA). Statistical significance was set at $p < 0.05$. Three sections from each film were analyzed for each mechanical property; for WCA, 5 different spots were measured. Therefore, these measurements were treated as technical replicates rather than independent experimental replicates.

RESULTS AND DISCUSSION

Structural Analysis

FTIR Analysis of Chickpea Starch

The FTIR spectrum of the extracted chickpea starch is shown in Figure 3. The characteristic absorption bands of starch confirm successful extraction and preservation of its chemical structure. These bands arise from the molecular vibrations of amylose and amylopectin, which are composed of glycosidic linkages, along with associated water molecules.

The broad absorption band at 3283 cm^{-1} is assigned to the O–H stretching vibration of hydroxyl groups involved in extensive intra- and intermolecular hydrogen bonding within the amylose and amylopectin chains. Similar hydroxyl stretching bands have been reported around 3400–3453 cm^{-1} for starches isolated from various botanical sources [37–40]. The bands at 2921 cm^{-1} and 1147 cm^{-1}correspond to the C–H stretching vibration and the CO stretching vibration of glucoside rings, respectively. These values are consistent with literature values of approximately 2923–2931 cm^{-1} reported for cassava and pejibaye starches [37].

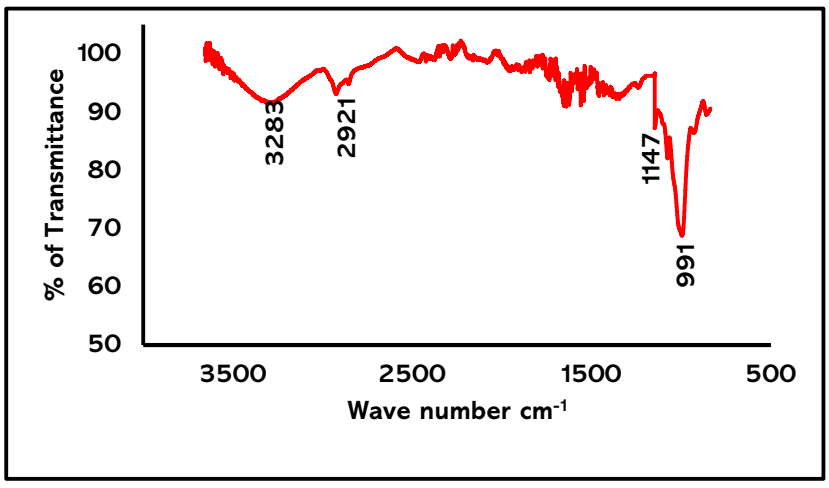


Figure 3. FTIR Spectra of chickpea starch.

A prominent absorption band at 991 cm^{-1} falls within the characteristic carbohydrate fingerprint region (1080–990 cm^{-1}) and is attributed to asymmetrical C–O–C vibration, axial C–O stretching, and skeletal vibrations of the starch backbone [39]. Weak absorptions below 950 cm^{-1} are generally associated with deformation vibrations of C–OH, C–CH, and O–CH groups, together with skeletal vibrations of the polysaccharide chain. Overall, the close agreement between the observed spectrum and previously reported starch spectra confirms the starch's native chemical structure [40].

SEM Analysis of Chickpea Starch

The SEM micrograph of the chickpea starch is presented in Figure 4. The starch granules exhibit predominantly spherical to oval morphology and the starch granules were approximately 10 μm in diameter, which is consistent with previous reports for chickpea starch, however, this value was estimated visually and was not determined through quantitative image analysis [41]. Most granules possess relatively smooth surfaces, although some show surface roughness, deformation, and partial fusion, likely resulting from the extraction and drying processes. Aggregation of granules into compact clusters is also observed, indicating inter-particle adhesion. Overall, the starch retains its characteristic granular morphology despite minor structural modifications. The observed granule size and morphology are comparable to those reported for starches from potato, corn, rice, and jackfruit. This suggests that the extracted chickpea starch possesses typical structural features suitable for food and biodegradable material applications [42–45].

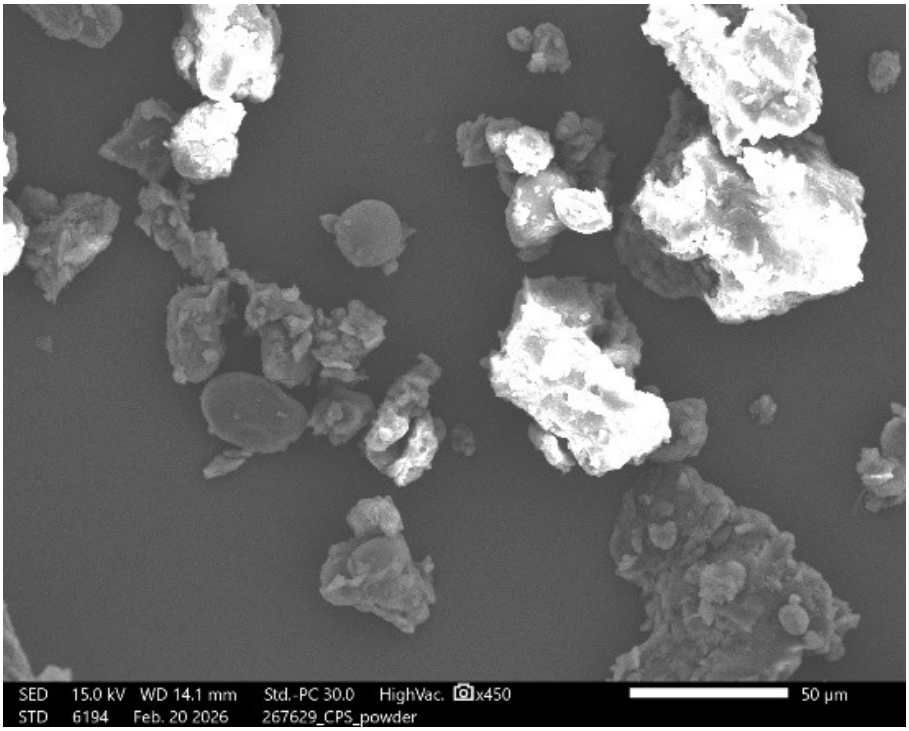


Figure 4. SEM image of chickpea starch.

TGA and DTG Analysis of Chickpea Starch

The thermal stability of the chickpea starch (CPS) was evaluated by thermogravimetric analysis (TGA), and the corresponding thermogram is presented in Figure 5A,B. The TGA curve exhibited two characteristic weight-loss stages. The initial weight loss below 267 °C was attributed to the evaporation of physically adsorbed and bound moisture without significant degradation of the starch structure. The major thermal degradation commenced at approximately 267 °C, where nearly 10% weight loss was observed, and continued up to 470 °C. This stage is associated with the depolymerization of amylose and amylopectin chains, dehydration reactions, fragmentation of glucopyranose rings, and formation of volatile degradation products [46]. At 600 °C, approximately 80% of the original mass had decomposed, leaving a small residue. The relatively high degradation onset temperature and broad decomposition range indicate that chickpea starch possesses excellent thermal stability, making it a suitable biopolymer for thermally processed film applications.

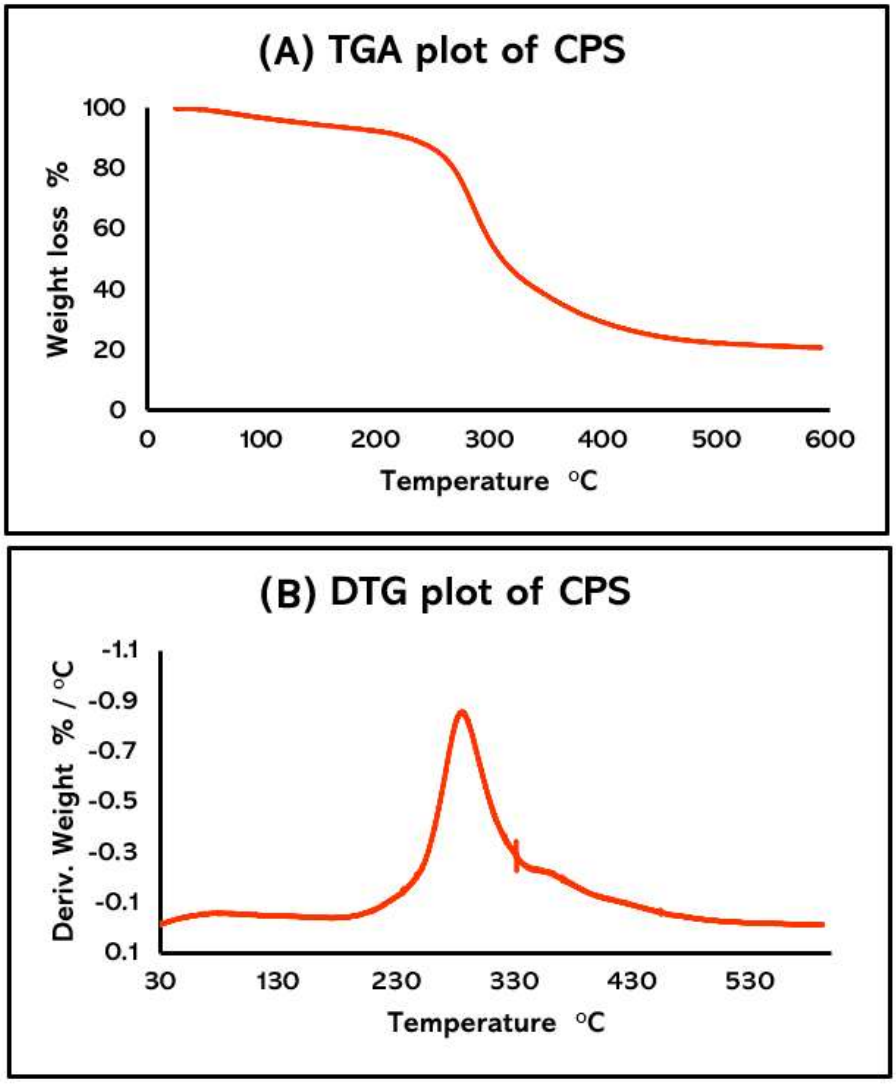


Figure 5. (A). TGA curve of chickpea starch. **(B)** DTG curve of chickpea starch.

Compared with starches obtained from other botanical sources, chickpea starch exhibited superior thermal stability. For example, pejibaye starch begins its major degradation at 251.7 °C and reaches maximum decomposition near 380 °C, with approximately 76.6% mass loss during the principal degradation stage [24]. Similarly, corn starch has been reported to initiate thermal degradation at approximately 220 °C [47], whereas rice starch begins degrading at around 210 °C, indicating lower thermal resistance than chickpea starch [48]. Likewise, cashew nut starch exhibits degradation beginning at approximately 174 °C, demonstrating considerably lower thermal stability [49]. The higher degradation onset temperature of chickpea starch (267 °C) suggests that its granules possess stronger intermolecular interactions and a more thermally resistant molecular architecture, which may be attributed to differences in amylose-to-amylopectin ratio, crystalline organization, granule morphology, and hydrogen-bonding density.

The enhanced thermal stability observed for chickpea starch is particularly advantageous for bio-based film production because it provides a wider processing window before thermal degradation occurs. Since film fabrication, gelatinization, extrusion, and hot-pressing operations are generally conducted below 200 °C, the degradation onset of 267 °C indicates that chickpea starch can withstand conventional thermal processing without significant structural decomposition [50]. Therefore, Chickpea starch represents a promising renewable biopolymer for developing the potential bio-based films.

FTIR Analysis of Synthesized Bio-based Films

The FTIR spectra of the chickpea starch-based films are presented in Figure 6. All formulations exhibited the characteristic absorption bands of starch, sodium alginate, and glycerol, CNC confirming the successful formation of a homogeneous polymer network. The broad absorption band centered at 3200–3400 cm^{-1} corresponds to the stretching vibration of hydroxyl (–OH) groups originating from starch, alginate, and glycerol [51]. The broadening and slight shift of this band compared with native starch indicates the establishment of extensive intermolecular hydrogen bonding among the polymer chains. Glycerol acts as a plasticizer by replacing part of the starch–starch and alginate–alginate hydrogen bonds with starch–glycerol and alginate–glycerol interactions, thereby enhancing chain mobility and flexibility [52].

The absorption bands near 2920–2940 cm^{-1} are assigned to the asymmetric stretching vibration of aliphatic C–H groups, while the band around 1640–1650 cm^{-1} is associated with the bending vibration of absorbed or bound water molecules within the hydrophilic polymer matrix [51]. Characteristic peaks in the 1410–1430 cm^{-1} region corresponds to the symmetric stretching vibration of carboxylate ($–COO^-$) groups of sodium alginate. The strong absorption band between 900 and 1100 cm^{-1} is attributed to C–O–C and C–O stretching vibrations of the polysaccharide

backbone and glycosidic linkages present in starch, alginate, and cellulose nanocrystals [51].

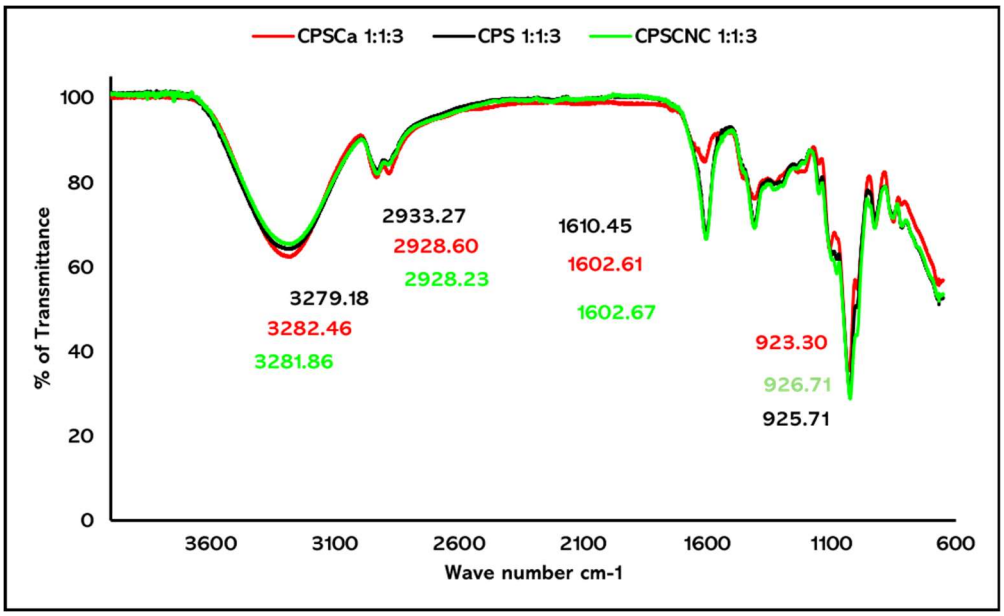


Figure 6. FTIR spectra of different formulations of bioplastics.

Following the incorporation of $CaCl_2$ and cellulose nanocrystals (CNC), slight shifts in the peak positions and intensities of the characteristic absorption bands were observed, indicating intermolecular interactions within the polymer matrix [53–56]. The broad O–H stretching band shifted from 3279.18 cm^{-1} for the CPS/SA/Gly (1:1:3) film to 3282.46 cm^{-1} for the CPSCa film and 3281.86 cm^{-1} for the CPSCNC film. Likewise, the C–H stretching vibration shifted from 2933.27 cm^{-1} (CPS) to 2928.60 cm^{-1} (CPSCa) and 2928.23 cm^{-1} (CPSCNC). The absorption band at 1610.45 cm^{-1} assigned to the asymmetric stretching vibration of carboxylate ($–COO^-$) groups and bound water shifted to 1602.61 cm^{-1} for CPSCa and 1602.67 cm^{-1} for CPSCNC. Additionally, the peak at 923.30 cm^{-1}, associated with glycosidic linkages in the polysaccharide backbone, shifted to 926.71 cm^{-1} and 925.71 cm^{-1}, respectively. These changes in peak position and intensity confirm strong molecular interactions within the film matrix. In the $CaCl_2$-containing films, the shifts are primarily attributed to ionic interactions between Ca^{2+} ions and the carboxylate groups of sodium alginate, resulting in the formation of the characteristic crosslinked network. In contrast, the CPSCNC films exhibit enhanced hydrogen bonding between the hydroxyl groups of CNC and the starch–alginate matrix. These intermolecular interactions improve polymer compatibility, strengthen the network structure, and enhance the mechanical properties, thermal stability, and water resistance of the developed bio-based films. This is reflected in their enhanced mechanical strength and thermal stability, as demonstrated by the tensile and TGA results.

Mechanical Properties

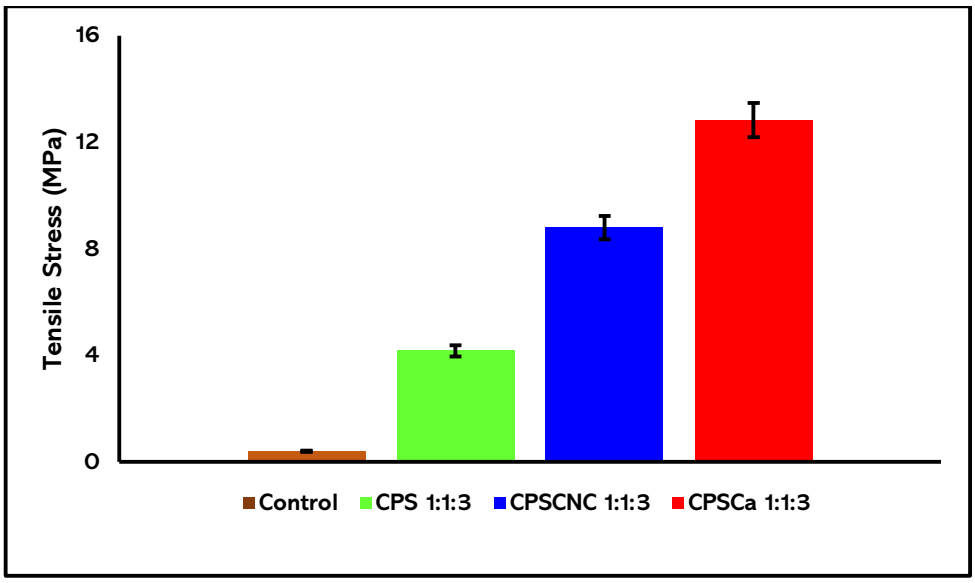
The mechanical properties of the developed bio-based films are shown in Figure 7. Incorporating chickpea starch (CPS), cellulose nanocrystals (CNC), and calcium chloride ($CaCl_2$) markedly altered the mechanical behavior of the sodium alginate (SA)-based films by modifying intermolecular interactions and the polymer matrix's network architecture.

The SA/Gly control film (Control 1:3) showed the poorest mechanical performance, with a tensile strength of approximately 0.4 ± 0.14 MPa, a Young's modulus of about 2.0 ± 1.07 MPa, and an elongation at break of only 26.88% ± 8.78%. The low tensile strength and stiffness indicate that the alginate network alone has limited load-bearing capacity under the selected formulation. Although glycerol acts as an efficient plasticizer by reducing intermolecular attractions between alginate chains, excessive chain mobility weakens cohesive forces within the matrix, resulting in poor resistance to tensile deformation.

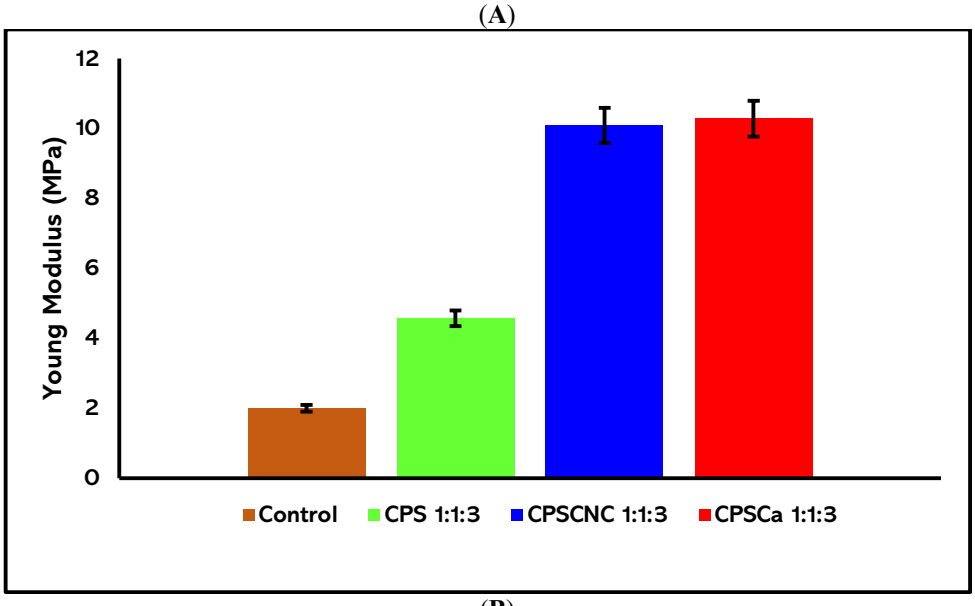
The incorporation of chickpea starch to produce the CPS 1:1:3 film significantly enhanced the mechanical properties. The tensile strength increased to approximately 4.16 ± 0.41 MPa, while the Young's modulus reached 4.6 ± 1.51 MPa, representing nearly a two-fold increase in stiffness compared with the control film. More remarkably, the elongation at break increased dramatically to approximately 373.84% ± 22.3%, indicating that the starch-containing film became both stronger and substantially more ductile. The improved mechanical performance of the CPS film stems from favorable intermolecular interactions between starch and sodium alginate. Both polymers contain abundant hydroxyl groups, which promote hydrogen bonding between adjacent polymer chains. These interactions foster close association between polymer chains and enhance interfacial compatibility between the two polysaccharides, yielding a more cohesive, interconnected polymer matrix. Such molecular interactions help distribute applied stress across the polymer network and reduce localized deformation. Meanwhile, glycerol forms additional hydrogen-bonding interactions with both polysaccharides, partially competing with polymer–polymer hydrogen bonding and increasing chain mobility. This plasticizing effect allows the polymer chains to rearrange under applied stress, improving flexibility, while the starch–alginate interactions help maintain matrix cohesion. Together, polymer–polymer interactions and glycerol-mediated plasticization improve the balance between tensile strength and flexibility in the CPS film.

The addition of cellulose nanocrystals produced the CPSCNC 1:1:3 film, which further improved the tensile strength to approximately 8.8 ± 0.60 MPa and increased the Young's modulus to nearly 10 ± 1.05 MPa, indicating a substantial enhancement in film stiffness. The improved mechanical performance of the CPSCNC film compared with the CPS film can be attributed to the reinforcing effect of CNCs within the starch–alginate matrix. The rigid nature and high aspect ratio of CNCs allow them

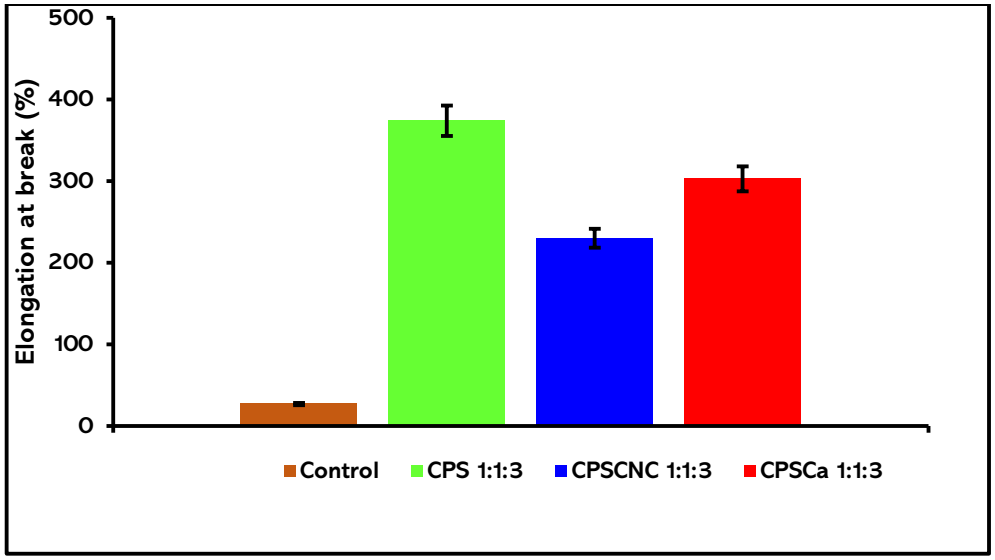
to act as reinforcing domains, while their surface hydroxyl groups can form hydrogen-bonding interactions with starch and alginate chains. These interactions improve interfacial adhesion between the nanocrystals and the polymer matrix, facilitating stress transfer under tensile loading. Furthermore, the incorporation of CNCs can restrict the relative movement of neighboring polymer chains, increasing resistance to deformation and improving the load-bearing capacity of the film. However, this restriction in chain mobility also limits polymer-chain rearrangement during stretching, resulting in a reduced elongation at break of approximately 230% ± 46.46%. Thus, CNC incorporation improves mechanical strength at the expense of some flexibility, consistent with the typical reinforcement behavior of nanocellulose in polysaccharide-based composites.



(A)



(B)



(**C**)

Figure 7. (A). Tensile stress of bio-based plastic at different formulations the linear model showed a statistically significant difference in tensile strength among the four film groups ($F_{3,7}$ = 143.5, $p < 0.001$), explaining 98.4% of the variation in tensile strength (R^2 = 0.984). Compared with the control group, tensile strength was significantly higher in CPS 1:1:3 (mean difference = 3.77 MPa, $p < 0.001$), CPSCNC 1:1:3 (mean difference = 8.40 MPa, $p < 0.001$), and CPSCa 1:1:3 (mean difference = 12.43 MPa, $p < 0.001$). The CPSCa 1:1:3 group showed the largest mean tensile strength, followed by CPSCNC 1:1:3, CPS 1:1:3, and Control. **(B).** Young's modulus of bio-based plastic at different formulations. The linear model showed a statistically significant difference in Young's modulus among the four film groups ($F_{3,7}$ = 30.58, $p < 0.001$) and explained 89.8% of the variation in Young's modulus (R^2 = 0.898). Compared with the control group, Young's modulus was significantly higher in CPS 1:1:3 (mean difference = 2.57 MPa, $p < 0.001$), CPSCNC 1:1:3 (mean difference = 8.09 MPa, $p < 0.001$), and CPSCa 1:1:3 (mean difference = 8.28 MPa, $p < 0.001$). **(C).** Elongation at break of bio-based plastic at different formulations the linear model showed a statistically significant difference in elongation at break among the four film groups ($F_{3,7}$ = 76.21, $p < 0.001$) and explained 95% of the variation in elongation at break (R^2 = 0.95). Compared with the control group, elongation at break was significantly higher in CPS 1:1:3 (mean difference = 348.84%, $p < 0.001$), CPSCNC 1:1:3 (mean difference = 230%, $p = 0.02$), and CPSCa 1:1:3 (mean difference = 276.94%, $p < 0.001$).

Among all formulations, the CPSCa 1:1:3 film exhibited the highest mechanical performance, with a tensile strength of approximately 12.8 ± 1.21 MPa and a Young's modulus slightly exceeding 10.28 ± 0.96 MPa. Compared with the CPS film, calcium incorporation resulted in more than a threefold increase in tensile strength while maintaining a relatively high elongation at break of approximately 302% ± 60.71%. The substantial improvement in the mechanical properties of the CPSCa film can be attributed primarily to Ca^{2+}-induced ionic interactions with the carboxylate groups of sodium alginate. Calcium ions can coordinate with carboxylate groups on adjacent alginate chains, forming interchain ionic junctions. These junctions provide additional physical constraints within the polymer matrix, limiting chain slippage and improving resistance to deformation under tensile loading. In parallel, hydrogen-bonding interactions between chickpea starch and alginate contribute to

intermolecular cohesion, further stabilizing the polymer matrix. The combined contribution of ionic junctions and hydrogen-bonding interactions therefore provides a more effective load-bearing structure than the uncrosslinked starch–alginate matrix. Despite the increased network constraints, the CPSCa film retained appreciable extensibility, with glycerol likely facilitating polymer-chain rearrangement and deformation under applied stress. This suggests that plasticization partially offsets the restriction in chain mobility imposed by ionic crosslinking. Overall, the simultaneous improvement in tensile strength and stiffness, together with the retention of considerable elongation, indicates that Ca^{2+} incorporation provides an effective reinforcement strategy for the starch–alginate matrix.

Overall, the mechanical properties obtained for the developed films are comparable to or superior to those reported for starch- and alginate-based films [57–60]. The significant improvement observed after $CaCl_2$ incorporation demonstrates that ionic crosslinking is a highly effective strategy for enhancing the structural performance of chickpea starch–alginate bio-based films while preserving sufficient flexibility for practical handling, processing, and end-use applications.

Morphological Analysis

SEM was used to examine the surface morphology of the chickpea starch-based bioplastic films, and the corresponding micrographs are presented in Figure 8. The control starch film exhibited a relatively smooth and continuous surface with no apparent cracks or phase separation, indicating good compatibility among chickpea starch, sodium alginate, and glycerol. After the incorporation of $CaCl_2$, the film maintained a compact and homogeneous morphology, suggesting uniform dispersion of the reinforcing components within the polymer matrix. No obvious pores, voids, or large agglomerates were observed, demonstrating effective blending and strong interfacial interactions among the film constituents. The dense microstructure is attributed to extensive hydrogen bonding between starch, alginate, glycerol, and Ca^{2+}induced ionic crosslinking of alginate, which promoted the formation of a stable polymer network.

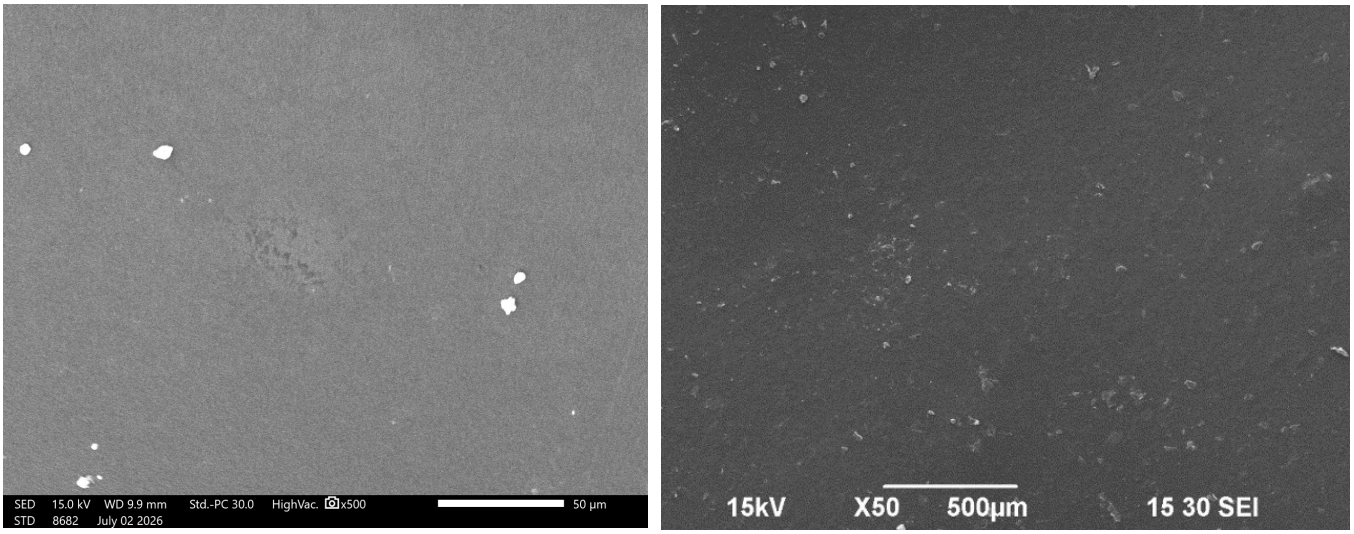
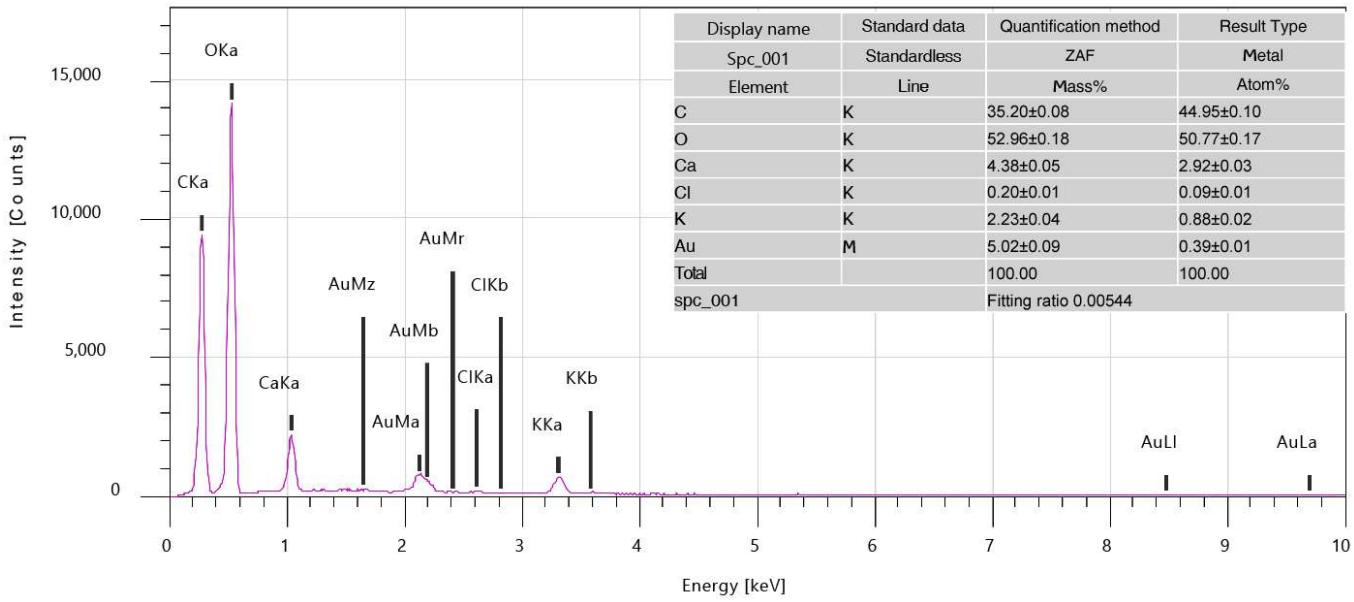


Figure 8. SEM image of CPS 1:1:3 (**left**), CPSCa 1:1:3 (**right**).

The EDS spectrum (Figure 9) confirmed the elemental composition of the starch–alginate–$CaCl_2$ composite. Carbon (35.20 wt% ± 0.08 wt%) and oxygen (52.96 wt% ± 0.18 wt%) were the predominant elements, corresponding to the carbohydrate backbone of starch and alginate. The presence of calcium (4.38 wt% ± 0.05 wt%) confirmed successful Ca^{2+} incorporation into the polymer matrix, indicating ionic interactions between calcium ions and alginate carboxylate groups. Trace chlorine (0.20 wt% ± 0.01 wt%) was attributed to residual chloride from $CaCl_2$, while potassium (2.23 wt% ± 0.04 wt%) likely originated from processing-related impurities. Gold peaks were associated with sputter coating during SEM preparation. The detection of calcium supports the formation of Ca^{2+}-mediated crosslinks, which may enhance intermolecular interactions and improve the structural stability of the bio-based film.



Display name	Standard data	Quantification method	Result Type
Spc_001	Standardless	ZAF	Metal
Element	Line	Mass%	Atom%
C	K	35.20±0.08	44.95±0.10
O	K	52.96±0.18	50.77±0.17
Ca	K	4.38±0.05	2.92±0.03
Cl	K	0.20±0.01	0.09±0.01
K	K	2.23±0.04	0.88±0.02
Au	M	5.02±0.09	0.39±0.01
Total		100.00	100.00
spc_001		Fitting ratio 0.00544	

Figure 9. EDS analysis of CPSCa 1:1:3.

Thermal Stability

The thermal stability of the CPS 1:1:3 and CPSCa 1:1:3 bio-based films was evaluated by thermogravimetric analysis (TGA), and derivative thermogravimetry (DTG) and the corresponding thermograms are shown in Figure 10. Both films exhibited a multistep degradation profile characteristic of starch–alginate-based biopolymer systems. The initial weight loss below approximately 150–180 °C was attributed to the evaporation of physically adsorbed and bound water, together with the partial volatilization of glycerol, without significant degradation of the polymer backbone.

For the CPS 1:1:3 film, the principal degradation began at approximately 159 °C, with an initial weight loss of about 8%. A rapid decomposition stage occurred around 291 °C, during which approximately 20% of the film's mass was lost, corresponding to the thermal degradation of starch and alginate via cleavage of glycosidic bonds, depolymerization of amylose and amylopectin, and decomposition of the polysaccharide backbone. At 600 °C, only about 10% residual mass remained, indicating extensive thermal decomposition of the polymer matrix.

In contrast, the CPSCa 1:1:3 film exhibited improved thermal stability following $CaCl_2$ incorporation. The onset of major degradation shifted to a higher temperature (173 °C), demonstrating that calcium ions delayed the thermal decomposition of the polymer network. Although the initial degradation reached approximately 15%, the principal degradation occurred at 291 °C with about 33% weight loss. More importantly, the Ca-crosslinked film retained approximately 21% residue at 600 °C, more than double that of the CPS film. This is because $CaCl_2$ is stable even at 600 °C [61].

The enhanced thermal stability of the CPSCa film is attributed to Ca^{2+}-mediated ionic crosslinking between the carboxylate groups of sodium alginate. This crosslinked network strengthens intermolecular interactions, restricts polymer chain mobility, and increases the energy required to break the polymer backbone during heating. Consequently, the calcium-crosslinked film exhibited greater resistance to thermal degradation and improved residual stability compared with the non-crosslinked CPS film.

From an application perspective, the improved thermal resistance of the CPSCa film is advantageous for edible bioplastic production, as it enhances processing stability during film casting, drying, heat sealing, and storage without compromising biodegradability [62]. The higher thermal stability also suggests improved resistance to thermal deformation during practical handling and food-packaging applications, making calcium-crosslinked chickpea starch–alginate films more suitable than the non-crosslinked formulation.

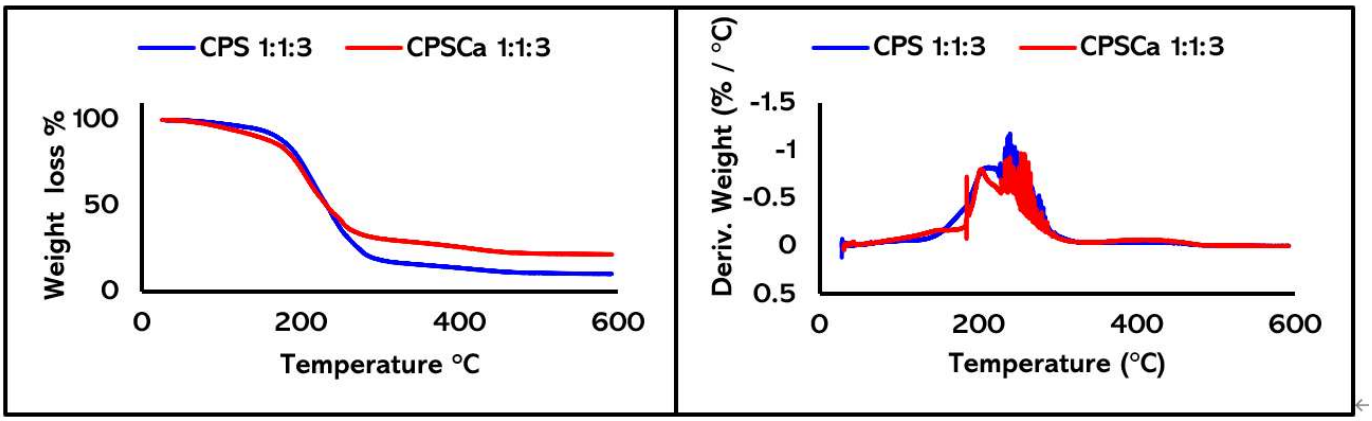


Figure 10. TGA (**left**) and DTG (**right**) curve of plastic films.

Water Vapor Permeability

Water vapor permeability (WVP) is a critical property governing the moisture barrier performance of biodegradable packaging materials. Water vapor permeability (WVP) quantifies the ability of a film to resist the transmission of water vapor and is expressed as the amount of water vapor passing through a unit area of film per unit time under a defined pressure gradient. Water vapor transport through polymeric films generally occurs via the solution–diffusion mechanism, which involves adsorption of water molecules onto the film surface, diffusion through the polymer matrix driven by the concentration gradient, and subsequent desorption from the opposite surface. The permeability is therefore governed by both the diffusivity of water molecules within the polymer network and their solubility in the film matrix [63,64].

As shown in Figure 11, of weight gain vs time plot, m = 0.8532, R^2 = 0.8996: therefore, using equation 4, CPSCa 1:1:3 edible film exhibited a WVP of 8.66 × 10^{-14} g·day^{-1}·m^{-1}·Pa^{-1}, whereas the commercial Ziploc sandwich bag (control) showed a WVP of 1.48× 10^{-16} g·day^{-1}·m^{-1}·Pa^{-1}. The difference in permeability reflects the distinct molecular structures of the two materials. The Ziploc sandwich bag, composed of hydrophobic polyethylene, provides an effective moisture barrier due to its dense, nonpolar polymer network, thereby exhibiting lower water vapor permeability. In contrast, the CPSCa film is based on hydrophilic polysaccharides containing abundant hydroxyl and carboxyl groups, which readily interact with water molecules and facilitate moisture diffusion.

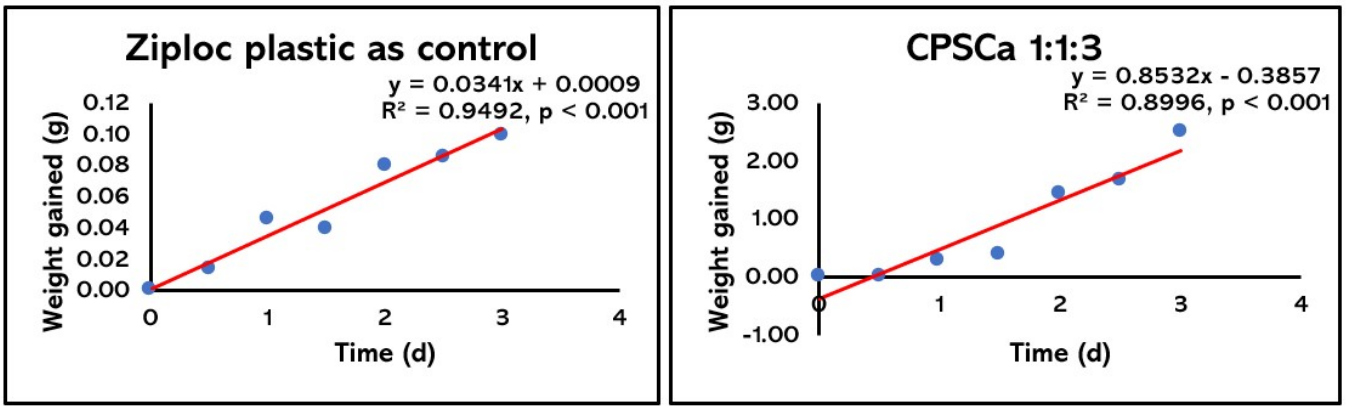


Figure 11. Weight gain as a function of time during water vapor permeability (WVP) measurements for the control (**left**) and CPSCa 1:1:3 bioplastic film (**right**). The weight gain increased with time in both the control and bio-based plastic film setups. The slope (m) of each linear regression represents the rate of weight gain over time. A lower slope for the plastic film compared with the control indicates that the film reduced water vapor transmission, suggesting better moisture barrier performance. The R^2 values indicate how well the linear regression fits the experimental data.

Despite the hydrophilic nature of chickpea starch, the incorporation of calcium chloride significantly improved the moisture barrier properties of the CPSCa film. Calcium ions form ionic crosslinks with the carboxylate groups of sodium alginate, which reduces the free volume within the polymer matrix and restricts the diffusion of water vapor. Furthermore, hydrogen bonding between chickpea starch and alginate contributes to a denser polymer structure, further limiting moisture transport through the film.

Although the WVP of the CPSCa film remained higher than that of the commercial polyethylene film, its barrier performance is adequate for edible packaging applications, where biodegradability, renewability, and food safety are prioritized over the extremely low permeability of conventional petroleum-based plastics. These findings suggest that calcium-crosslinked chickpea starch–alginate films offer a favorable balance between moisture barrier performance and environmental sustainability, making them promising candidates for edible food packaging.

Water Contact Angle

Water contact angle (WCA) is an important indicator of the surface wettability and moisture resistance of bio-based films. It reflects the interaction between water droplets and the film surface, where a higher contact angle indicates lower wettability and improved resistance to water penetration. As shown in Figures 12 and 13, the CPSCa 1:1:3 film exhibited a water contact angle of 82.92° ± 1.65°, whereas the commercial Ziploc sandwich bag and Walmart bag exhibited higher contact angles of 101.1° and 93.59°, respectively. The differences in WCA can be attributed primarily to variations in polymer composition and surface chemistry.

The CPSCa film contains chickpea starch and sodium alginate, both of which contain abundant hydroxyl groups, while alginate also contains carboxylate groups. These polar functional groups can interact with water molecules through hydrogen bonding, resulting in greater surface wettability than that of conventional polyethylene-based packaging materials. In comparison, polyethylene has a predominantly nonpolar hydrocarbon structure with limited affinity for water, which accounts for the higher contact angles observed for the commercial bags. The slightly lower WCA of the Walmart bag compared with the Ziploc bag may reflect differences in polymer composition, additives, surface treatments, or surface morphology.

The CPSCa film exhibited a contact angle below 90°, indicating that its surface remained moderately hydrophilic despite the incorporation of $CaCl_2$. Calcium ions can interact ionically with carboxylate groups of alginates, potentially reducing the availability or mobility of some hydrophilic polymer segments at the surface and modifying the surface organization of the polymer network. However, the abundant hydroxyl groups in starch and alginate continue to contribute to water affinity. Therefore, the measured contact angle represents the combined influence of the hydrophilic polysaccharide components, ionic interactions, and surface characteristics. Although the CPSCa film showed lower surface water repellency than the commercial bags, its contact angle indicates that the film is less readily wet than would be expected for an untreated, highly hydrophilic polysaccharide surface.

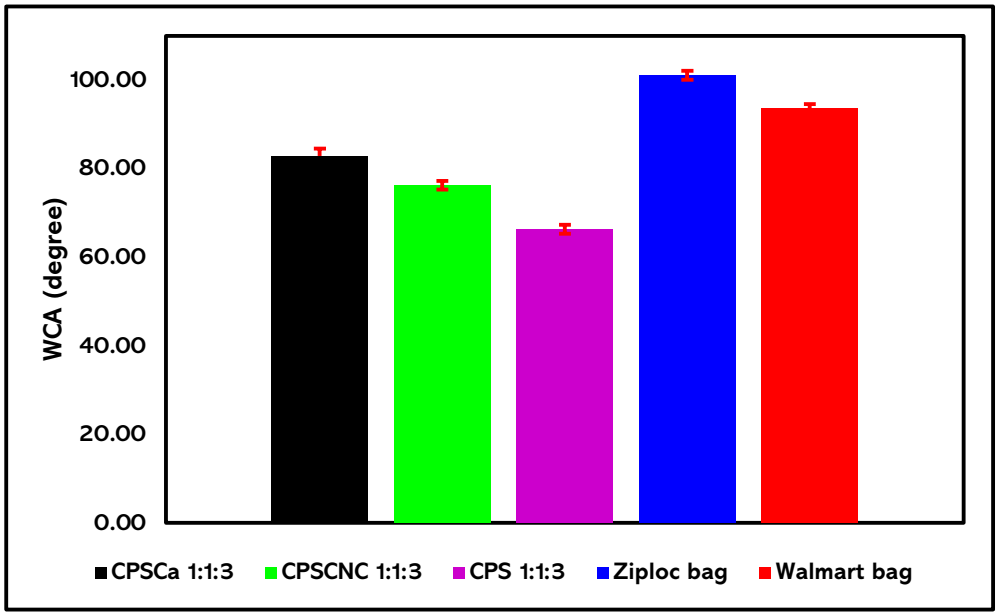


Figure 12. Water contact angles of bio-based plastics at different formulations and controls. The linear model showed a statistically significant difference in water contact angle among the four film groups and Walmart, Ziploc bag ($F_{4,15}$ = 91.09, $p < 0.001$) and explained 94% of the variation in elongation at break (R^2 = 0.94). Compared with the CPS 1:1:3, WCA was significantly higher in CPSCa 1:1:3 (mean difference = 16.58%, $p < 0.001$), CPSCNC 1:1:3 (mean difference = 9.93, $p < 0.001$), Walmart bag (mean difference = 27.26, $p < 0.001$), and Ziploc sandwich bag (mean difference = 34.76, $p < 0.001$).

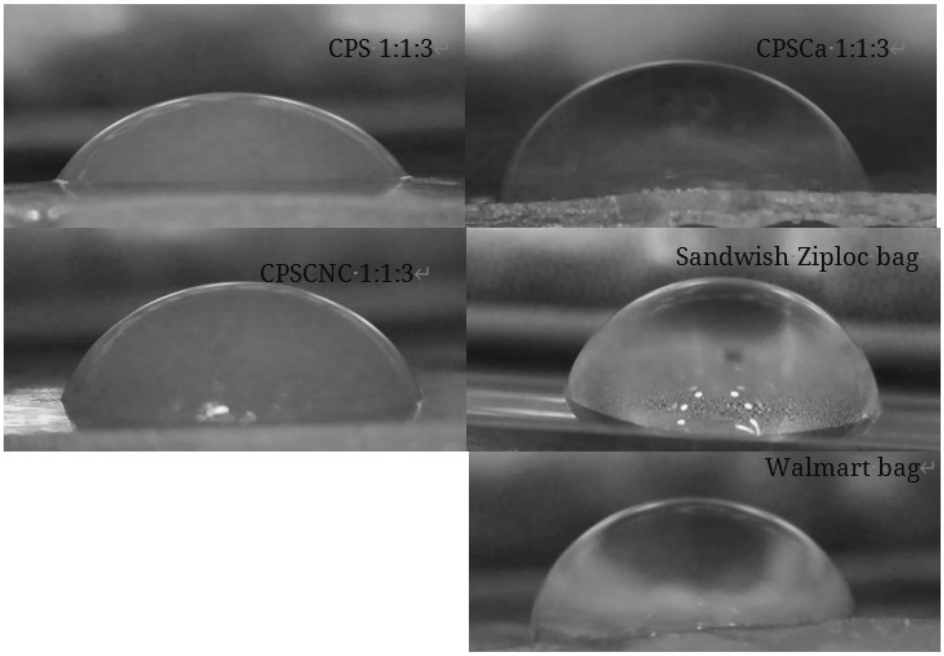


Figure 13. Water Contact Angle images.

Film Density

The densities of the developed bio-based films are presented in Table 1. The CPS 1:1:3 film exhibited the lowest density, 0.93 ± 0.12 g/cm^3, followed by the CPSCNC 1:1:3 film, 1.217 ± 0.16 g/cm^3, while the CPSCa 1:1:3 film showed the highest density, 1.274 ± 0.14 g/cm^3. The progressive increase in density demonstrates the significant influence of reinforcing agents on the internal structure and packing efficiency of the polymer matrix.

The relatively low density of the CPS film is attributed to a network stabilized primarily by hydrogen bonding between chickpea starch and sodium alginate, resulting in greater free volume and a less compact polymer structure. Incorporation of cellulose nanocrystals increased the density to 1.217 g/cm^3 because the highly crystalline CNCs acted as rigid nanofillers, occupying micro voids and promoting stronger intermolecular hydrogen bonding, thereby producing a more compact and homogeneous matrix. The highest density was observed for the CPSCa film, where Ca^{2+} ions formed ionic crosslinks with the carboxylate groups of sodium alginate. This ionic crosslinking reduced the free volume between polymer chains and promoted closer molecular packing, resulting in the densest film among all formulations

The observed density trend (CPS < CPSCNC < CPSCa) is consistent with the tensile, thermal, and barrier property results, where the calcium-crosslinked film exhibited the greatest mechanical strength, thermal stability, and moisture resistance. Furthermore, the density values obtained (0.93–1.274 g/cm^3) fall within the range commonly reported for starch-based biodegradable and edible films, indicating that the developed films possess sufficient structural integrity while remaining lightweight [65]. The high density of the CPSCa film suggests the formation of a

compact and well-organized polymer network, making it particularly suitable for sustainable edible food-packaging applications.

Film's Transparency

The transparency of bio-based films is an important optical property that influences consumer acceptance and allows visual inspection of packaged foods. As presented in Table 3, the CPSCa 1:1:3 film exhibited a transparency value of 2.26/mm, indicating good optical clarity while maintaining the structural integrity of the bioplastic. Although the film was less transparent than conventional polyethylene films, 2.90/mm, this difference is expected because polysaccharide-based films possess a hydrophilic polymer network and greater thickness, which increase light scattering [66,67]. In addition, CPSCa has lower transparency than CPS film. This is because the incorporation of calcium ions can promote ionic crosslinking within the starch–alginate matrix, producing localized microstructural heterogeneity that slightly reduces light transmission [68].

Notably, the transparency of the CPSCa film was superior to several previously reported starch-based biodegradable films. For example, Mulyono et al. (2015) [69]. reported a transparency value of 3.13 for tapioca starch-based films, whereas the CPSCa film developed in this study exhibited a considerably lower value (2.26/mm), indicating lower transparency. The improved optical clarity may be attributed to the good compatibility between chickpea starch and sodium alginate, together with the formation of a homogeneous calcium-crosslinked polymer network that minimizes phase separation.

Table 3. Film transparency of the plastic with control.

Sample title	Transmittance %	Thickness (mm)	Transparency (/mm)
SA Control	82.4	0.56	3.42 ± 0.154
CPS 1:1:3	44	0.32	5.14 ± 0.132
CPSCa 1:1:3	42.6	0.72	2.26 ± 0.124
Ziploc sandwich bag	89.23	0.2	9.75 ± 0.112
Conventional Polyethylene bag	-	-	2.9

CONCLUSIONS

A sustainable film based on chickpea starch and sodium alginate was successfully fabricated via $CaCl_2$-mediated ionic crosslinking. Structural characterization by FTIR, SEM, and EDS analysis provided evidence of the incorporation of Ca^{2+} and the formation of a compact, homogeneous polymer network. This structural reinforcement was reflected in the mechanical properties, with the CPSCa 1:1:3 film exhibiting the highest tensile strength (~13 MPa) and Young's modulus (~10.5 MPa), and in the TGA and DTG analysis (degradation starts at 173 °C, major degradation starts at 291 °C, ~21% residue left at 600 °C), which showed enhanced thermal stability and a higher residual mass than the non-crosslinked film. Furthermore, the higher density (~1.3 g/cm^3), moderate water vapor

permeability (8.66×10^{-14} g·day^{-1}·m^{-1}·Pa^{-1}), moderate water contact angle (82°), and improved optical transparency (~2.3/mm) indicate a dense matrix with favorable moisture barrier performance while maintaining good visual clarity. Collectively, these findings demonstrate that calcium-mediated crosslinking effectively overcomes the inherent limitations of conventional starch-based films, producing a bioplastic with balanced mechanical, thermal, barrier, and optical properties. Therefore, the CPSCa 1:1:3 film shows promise as a bio-based material for potential short-term packaging of dry foods and other suitable food products. However, further studies on biodegradation, migration, food-contact safety, sensory acceptability, and edibility are necessary before it can be considered a safe, biodegradable, and edible alternative to conventional petroleum-based plastics.

LIMITATIONS AND FUTURE ASPECTS

This study focused on the physicochemical, mechanical, thermal, barrier, and structural properties of the developed bio-based film under laboratory conditions. The starting chickpea starch was not characterized for amylose content, purity, residual protein, particle-size distribution, or crystalline structure by XRD, which may influence film performance and $CaCl_2$-mediated crosslinking. Edibility, long-term storage stability, food-contact performance, sensory evaluation, migration behavior, and large-scale processing were not investigated and therefore require further study before commercial application. Future work should focus on evaluating the film with real food products under practical storage conditions, conducting food safety and migration studies, incorporating natural functional additives to develop active edible packaging, and assessing industrial-scale production and economic feasibility to facilitate commercialization.

DATA AVAILABILITY

The dataset of the study is available from the authors upon reasonable request.

AUTHOR CONTRIBUTIONS

Methodology, writing—original draft preparation, writing—review and editing, MARB; Conceptualization and Manuscript Review, IZ; Supervision and Funding Acquisition, KH; Lab and experimental support, BW and LH; English correction and critical review, MK. All authors have read and approved the final published version of the manuscript.

CONFLICTS OF INTEREST

The authors declare no conflicts of interest.

FUNDING

This work was conducted at Mayville State University and partially funded by NSF EPSCoR Track-1 ND-ACES (OIA # 1946202) and NSF EPSCoR ECORE RII SPARK-ND (OIA # 2438111).

ACKNOWLEDGMENTS

The authors gratefully acknowledge the financial support received for this research, as well as the facilities and technical assistance provided by the NDSU Electron Microscopy Core, which were instrumental in the characterization of the materials studied. The authors also acknowledge the Department of Chemistry at the University of North Dakota (UND) and the Department of Mechanical Engineering, including the Polymer and Coatings Program at North Dakota State University (NDSU), for their valuable contributions to the characterization aspects of this research. We are especially thankful Brian Folt, assistant unit leader, Nevada Cooperative and Wildlife Research Unit, for his contribution to statistical analysis.

REFERENCES

1. Sharma S, Chatterjee S. Microplastic pollution, a threat to marine ecosystem and human health: a short review. Environ Sci Pollut Res. 2017;24(27):21530-47. doi: 10.1007/s11356-017-9910-8
2. Andrady AL. Persistence of plastic litter in the oceans. In: Bergmann M, Gutow L, Klages M, editors. Marine Anthropogenic Litter. Cham (Switzerland): Springer International Publishing; 2015. p. 57-72. doi: 10.1007/978-3-319-16510-3_3
3. Geyer R, Jambeck JR, Law KL. Production, use, and fate of all plastics ever made. Sci Adv. 2017;3(7):e1700782. doi: 10.1126/sciadv.1700782
4. Sarker NC, Badsha MAR, Hillukka G, Holter B, Kjelland M, Hossain K. Pyrolyzed biochar from agricultural byproducts: synthesis, characterization, and application in water pollutants removal. Processes. 2025;13(5):1358. doi: 10.3390/pr13051358
5. Rana ZH, Mahmud MS, Alam MK. Is plant protein-based meat the future? Exploring recent advances, opportunities, and challenges. Food Bioprocess Technol. 2026;19(2):79. doi: 10.1007/s11947-025-04143-7
6. Matloob A, Ayub H, Mohsin M, Ambreen S, Khan FA, Oranab S, et al. A review on edible coatings and films: advances, composition, production methods, and safety concerns. ACS Omega. 2023;8(32):28932-44. doi: 10.1021/acsomega.3c03459
7. Han JH. Chapter 9-Edible films and coatings: a review. In: Han JH, editor. Innovations in Food Packaging. 2nd ed. San Diego (CA, US): Academic Press; 2014. p. 213-55. doi: 10.1016/B978-0-12-394601-0.00009-6
8. Dallaev R, Papež N, Allaham MM, Holcman V. Biodegradable polymers: properties, applications, and environmental impact. Polymers. 2025;17(14):1981. doi: 10.3390/polym17141981

9. LI WC, TSE HF, FOK L. Plastic waste in the marine environment: a review of sources, occurrence and effects. Sci Total Environ. 2016;566-567:333-49. doi: 10.1016/j.scitotenv.2016.05.084
10. Dongowski GRL. WHISTLER and JN BEMILLER: Carbohydrate chemistry for food scientists. Food Nahr. 1997;41(5):318. doi: 10.1002/food.19970410523
11. Pires AF, Díaz O, Cobos A, Pereira CD. A review of recent developments in edible films and coatings-Focus on whey-based materials. Foods. 2024;13(16):2638. doi: 10.3390/foods13162638
12. Esfandiari Z, Hassani B, Sani IK, Talebi A, Mohammadi F, Zomorodi S, et al. Characterization of edible films made with plant carbohydrates for food packaging: a comprehensive review. Carbohydr Polym Technol Appl. 2025;11:100979. doi: 10.1016/j.carpta.2025.100979
13. Gadhave RV, Das A, Mahanwar PA, Gadekar PT. Starch based bio-plastics: the future of sustainable packaging. Open J Polym Chem. 2018;8(2):21-33. doi: 10.4236/ojpchem.2018.82003
14. Sul JAI do, Costa MF. The present and future of microplastic pollution in the marine environment. Environ Pollut. 2014;185:352-64. doi: 10.1016/j.envpol.2013.10.036
15. Jørgensen HF, Fisher AG. Can controversies be put to REST? Nature. 2010;467(7311):E3-E4. doi: 10.1038/nature09305
16. Li K, Zhu J, Guan G, Wu H. Preparation of chitosan-sodium alginate films through layer-by-layer assembly and ferulic acid crosslinking: film properties, characterization, and formation mechanism. Int J Biol Macromol. 2019;122:485-92. doi: 10.1016/j.ijbiomac.2018.10.188
17. The DP, Debeaufort F, Voilley A, Luu D. Biopolymer interactions affect the functional properties of edible films based on agar, cassava starch and arabinoxylan blends. J Food Eng. 2009;90(4):548-58. doi: 10.1016/j.jfoodeng.2008.07.023
18. Seale R, Morris ER, Rees DA. Interactions of alginates with univalent cations. Carbohydr Res. 1982;110(1):101-12. doi: 10.1016/0008-6215(82)85029-5
19. Draget KI, Skjåk-Bræk G, Smidsrød O. Alginate based new materials. Int J Biol Macromol. 1997;21(1):47-55. doi: 10.1016/S0141-8130(97)00040-8
20. Mørch YA, Donati I, Strand BL, Skjåk-Bræk G. Effect of Ca^{2+}, Ba^{2+}, and Sr^{2+} on alginate microbeads. Biomacromolecules. 2006;7(5):1471-80. doi: 10.1021/bm060010d
21. Liu Y, Li J, Liang Z, Wang J, Pan Q. Preparation of double cross-linked starch/CaCl2/PVA conductive hydrogel for flexible solid-state supercapacitor. Int J Biol Macromol. 2025;320:145908. doi: 10.1016/j.ijbiomac.2025.145908
22. Skoric ML, Lukic I, Pantic M, Krusic MK, Novak Z, Milovanovic S. Biopolymer aerogels: structural and functional tailoring of starch/sodium alginate networks. Int J Biol Macromol. 2025;309:142774. doi: 10.1016/j.ijbiomac.2025.142774
23. Jost V, Reinelt M. Effect of Ca^{2+} induced crosslinking on the mechanical and barrier properties of cast alginate films. J Appl Polym Sci. 2018;135(5):45754. doi: 10.1002/app.45754

24. Neto BAdM, Fernandes BS, Junior CCMF, Franco M, Bonomo RCF, De Almeida PF, et al. Thermal-morphological characterisation of starch from peach-palm (Bactris gasipaes Kunth) fruit (pejibaye). Int J Food Prop. 2017;20(5):1007-15. doi: 10.1080/10942912.2016.1192645
25. Silva GMD, Veloso CM, Santos LS, Melo Neto BAd, Fontan RDCI, Bonomo RCF. Extraction and characterization of native starch obtained from the inhambu tuber. J Food Sci Technol. 2020;57(5):1830-9. doi: 10.1007/s13197-019-04216-4
26. Sarıkaya S, İnanlar B, Younis HGR, Zhao G, Ye F. Chickpea (Cicer arietinum Linn.) starch: extraction, composition, structure, properties, modifications and food applications. Grain Oil Sci Technol. 2025;8(2):118-36. doi: 10.1016/j.gaost.2025.03.003
27. Md Sultan Mahmud. Enhancing resin composite using nanoparticle embedded jute fiber and exploring plant polymer for biomedical applications [dissertation]. Grand Forks (ND, US): University of North Dakota; 2023. doi: 10.13140/RG.2.2.27329.21604
28. Hossain AR, Mahmud MS, Koistinen K, Davisson G, Roeges B, Boechler H, et al. Wheat bran polymer scaffolds: supporting triple-negative breast cancer cell growth and development. Bioengineering. 2025;12(6):568. doi: 10.3390/bioengineering12060568
29. Azmi NN, Ab Patar MNA, Mohd Noor SNA, Mahmud J. Testing standards assessment for silicone rubber. Proceedings of the 2014 International Symposium on Technology Management and Emerging Technologies; 2014 May 27-29; Bandung, Indonesia.
30. Cazón P, Morales-Sanchez E, Velazquez G, Vázquez M. Measurement of the water vapor permeability of chitosan films: a laboratory experiment on food packaging materials. J Chem Educ. 2022;99(6):2403-8. doi: 10.1021/acs.jchemed.2c00449
31. Gennadios A, Weller CL, Gooding CH. Measurement errors in water vapor permeability of highly permeable, hydrophilic edible films. J Food Eng. 1994;21(4):395-409. doi: 10.1016/0260-8774(94)90062-0
32. Ali MEA, Ahmed F, Ersan MS. The interplay between per- and polyfluoroalkyl substances removal and flux in direct contact membrane distillation. Desalination. 2026;619:119578. doi: 10.1016/j.desal.2025.119578
33. Baba EM, Cansoy CE, Zayim EO. Optical and wettability properties of polymers with varying surface energies. Appl Surf Sci. 2015;350:115-20. doi: 10.1016/j.apsusc.2015.02.150
34. Liu D, Chen P, Mu J, Yu Q, Lu C. Improvement and mechanism of interfacial adhesion in PBO fiber/bismaleimide composite by oxygen plasma treatment. Appl Surf Sci. 2011;257(15):6935-40. doi: 10.1016/j.apsusc.2011.03.035
35. Badsha MAR, Kjelland M, Ulven C, Hossain K. Arabinoxylan-based bioplastic from wheat bran: a promising replacement for synthetic plastics. Polymers. 2025;17(18):2488. doi: 10.3390/polym17182488
36. Badsha MAR, Kjelland M, Ulven C, Zaman IA, Hossain K. Biodegradable starch-based bioplastic from chickpea: a green alternative to conventional plastics. Processes. 2026;14(18):2892. doi: 10.3390/pr14182892

37. Valencia GA, Moraes ICF, Lourenço RV, Bittante AMQB, Sobral PJD. A physicochemical, morphological, and functional properties of flour and starch from peach palm (Bactris gasipaes K.) fruit. Starch-Starke. 2015;67(1-2):163-73. doi: 10.1002/star.201400097
38. Melo Neto BAd, Barbosa AA, Leite CXDS, Almeida PFD, Bonomo RCF, Pontes KV. Chemical composition and functional properties of starch extracted from the pejibaye fruit (Bactris gasepaes Kunt.). Acta Sci Technol. 2015;37(1):105. doi: 10.4025/actascitechnol.v37i1.20740
39. Sandle NK, Verma OPS, Varma IK. Thermal characterization of starch-g-acrylonitrile copolymers. Thermochim Acta. 1987;115:189-98. doi: 10.1016/0040-6031(87)88365-X
40. Mrozek MF, Weaver MJ. Detection and identification of aqueous saccharides by using surface-enhanced Raman spectroscopy. Anal Chem. 2002;74(16):4069-75. doi: 10.1021/ac020115g
41. Leonel M. Análise da forma e tamanho de grânulos de amidos de diferentes fontes botânicas. Cienc Tecnol Aliment. 2007;27(3):579-88.
42. Salgado SM, Guerra NB, Andrade SAC, Livera AVS. Caracterização físico-química do grândulo do amido do feijão caupi. Cienc Tecnol Aliment. 2005;25(3):525-30. doi: 10.1590/S0101-20612005000300022
43. Oliveira TMD, Pirozi MR, Borges JTDS, Germani R, Fontes MPF. Caracterização do amido de grão-de-bico (Cicer arietinum L.). Bol Cent Pesqui Process Aliment. 2009;27(1). doi: 10.5380/cep.v27i1.14947
44. Hernandez-Uribe JP, Agama-Acevedo E, Gonzalez-Soto RA, Bello-Pérez LA, Vargas-Torres A. Isolation and characterization of Mexican chayote tuber (Sechium edule Sw.) starch. Starch-Starke. 2011;63(1):32-41. doi: 10.1002/star.201000078
45. Weber FH, Collares-Queiroz FP, Chang YK. Caracterização físico-química, reológica, morfológica e térmica dos amidos de milho normal, ceroso e com alto teor de amilose. Cienc Tecnol Aliment. 2009;29(4):748-53. doi: 10.1590/S0101-20612009000400008
46. Aggarwal P, Dollimore D. A thermal analysis investigation of partially hydrolyzed starch. Thermochim Acta. 1998;319(1-2):17-25. doi: 10.1016/S0040-6031(98)00355-4
47. Liu X, Yu L, Liu H, Chen L, Li L. Thermal decomposition of corn starch with different amylose/amylopectin ratios in open and sealed systems. Cereal Chem. 2009;86(4):383-5. doi: 10.1094/CCHEM-86-4-0383
48. Fabian C, Ayucitra A, Ismadji S, Ju YH. Isolation and characterization of starch from defatted rice bran. J Taiwan Inst Chem Eng. 2011;42(1):86-91. doi: 10.1016/j.jtice.2010.03.013
49. Yuliana M, Truong CT, Huynh LH, Ho QP, Ju YH. Isolation and characterization of protein isolated from defatted cashew nut shell: influence of pH and NaCl on solubility and functional properties. LWT Food Sci Technol. 2014;55(2):621-6. doi: 10.1016/j.lwt.2013.10.022

50. Chen J, Wang X, Long Z, Wang S, Zhang J, Wang L. Preparation and performance of thermoplastic starch and microcrystalline cellulose for packaging composites: extrusion and hot pressing. Int J Biol Macromol. 2020;165:2295-302. doi: 10.1016/j.ijbiomac.2020.10.117
51. Saleh HM, Albukhaty S, Al-Karagoly H, Sulaiman GM, Gharbavi M. Optimized alginate-glycerol nano-hydrogel composites for enhanced Methylene Blue removal: kinetic and isotherm analysis. J Clust Sci. 2025;36(5):162. doi: 10.1007/s10876-025-02889-w
52. López OV, Ninago MD, Lencina MMS, García MA, Andreucetti NA, Ciolino AE, et al. Thermoplastic starch plasticized with alginate-glycerol mixtures: melt-processing evaluation and film properties. Carbohydr Polym. 2015;126:83-90. doi: 10.1016/j.carbpol.2015.03.030
53. Parit M, Jiang Z. Cellulose nanocrystal films: effect of electrolyte and lignin addition on self-assembly, optical, and mechanical properties. Cellulose. 2023;30(15):9405-23. doi: 10.1007/s10570-023-05464-6
54. Abdel-Hakim A, Mourad R. Nanocellulose and its polymer composites: preparation, characterization, and applications. Russ Chem Rev. 2023;92(4):RCR5076. doi: 10.57634/RCR5076
55. Vanitha D, Bahadur SA, Nallamuthu N, Shunmuganarayanan A, Manikandan A. Studies on conducting polymer blends: synthesis and characterizations of PVA/PVP doped with $CaCl_2$. J Nanosci Nanotechnol. 2018;18(3):1723-9. doi: 10.1166/jnn.2018.14215
56. Mousavi E, Manafi S, Mirjalili F. In situ synthesis and characterization of antibacterial sodium alginate-silver nanocomposite films incorporated with eucalyptus oil for food packaging applications. Ind Crops Prod. 2026;242:122943. doi: 10.1016/j.indcrop.2026.122943
57. Al-Hassan AA, Norziah MH. Starch-gelatin edible films: water vapor permeability and mechanical properties as affected by plasticizers. Food Hydrocoll. 2012;26(1):108-16. doi: 10.1016/j.foodhyd.2011.04.015
58. Costa MJ, Marques AM, Pastrana LM, Teixeira JA, Sillankorva SM, Cerqueira MA. Physicochemical properties of alginate-based films: effect of ionic crosslinking and mannuronic and guluronic acid ratio. Food Hydrocoll. 2018;81:442-50. doi: 10.1016/j.foodhyd.2018.03.014
59. Fazilah A, Maizura M, Abd Karim A, Bhupinder K, Rajeev B, Uthumporn U, et al. Physical and mechanical properties of sago starch-alginate films incorporated with calcium chloride. Int Food Res J. 2011;18(3):1027-34.
60. Mukaila T, Adeniyi A, Bello I, Sarker NC, Monono E, Hammed A. Optimizing film mechanical and water contact angle properties via PLA/starch/lecithin concentrations. Clean Circ Bioeconomy. 2024;8:100095. doi: 10.1016/j.clcb.2024.100095
61. Jiang X, Jiang T, Gan L, Zhang X, Dai H, Zhang X. The plasticizing mechanism and effect of calcium chloride on starch/poly (vinyl alcohol) films. Carbohydr Polym. 2012;90(4):1677-84. doi: 10.1016/j.carbpol.2012.07.050
62. Auras R, Harte B, Selke S. An overview of polylactides as packaging materials. Macromol Biosci. 2004;4(9):835-64. doi: 10.1002/mabi.200400043

63. Figura LO, Teixeira AA. Food physics: physical properties—measurement and applications. Berlin (Germany): Springer-Verlag; 2007.
64. Robertson GL. Food packaging. Boca Raton (FL, US): CRC Press; 2016. doi: 10.1201/b21347
65. Zhang Y, Liu Z, Han J. Starch-based edible films. In: Environmentally Compatible Food Packaging. Elsevier; 2008. p. 108-36. doi: 10.1533/9781845694784.1.108
66. Bertuzzi MA, Armada M, Gottifredi JC. Physicochemical characterization of starch based films. J Food Eng. 2007;82(1):17-25. doi: 10.1016/j.jfoodeng.2006.12.016
67. Ancy A, Lazar M, Saritha Chandran A, Ushamani M. Development of ecofriendly and sustainable bioplastics from cassava starch: tailoring the properties using nanoparticles. Sustain Chem Pharm. 2024;37:101377. doi: 10.1016/j.scp.2023.101377
68. Katileviciute A, Plakys G, Budreviciute A, Onder K, Damiati S, Kodzius R. A sight to wheat bran: high value-added products. Biomolecules. 2019;9(12):887. doi: 10.3390/biom9120887
69. Mulyono N, Suhartono MT, Angelina S. Development of bioplastic based on cassava flour and its starch derivatives for food packaging. J Harmon Res Appl Sci. 2015;3:125-33.

How to cite this article:
Badsha MAR, Weiers B, Hoeft L, Kjelland M, Zaman I, Hossain K. Potential Sustainable Edible Packaging from Chickpea Starch–Alginate Bioplastic. J Sustain Res. 2026;8(4):e260094. https://doi.org/10.20900/jsr20260094.